© 2001 The Chemical Society of Japan

Mass-Spectrometric Study on Ion-Molecule Reactions of CH_5^+, $C_2H_5^+$, and $C_3H_5^+$ with C_8–C_{18} 1-Olefins in an Ion Trap

Yuki Tanaka and Masaharu Tsuji[*,†]

Department of Applied Science for Electronics and Materials, Graduate School of Engineering Sciences, Kyushu University, Kasuga, Fukuoka 816-8580

†Institute of Advanced Material Study, Kyushu University, Kasuga, Fukuoka 816-8580

(Received November 24, 2000)

Chemical ionization of 1-olefins (C_xH_{2x}: x = 8–18) by the CH_5^+, $C_2H_5^+$, and $C_3H_5^+$ ions has been studied under a reactant-ion selective mode of an ion-trap type of GC/MS. In all the reactions, alkyl $C_yH_{2y+1}^+$ (y = 3–x) and alkenyl $C_yH_{2y-1}^+$ (y = 3–x) ions were observed. For long-chain reagents (x = 11–18), the $C_yH_{2y+1}^+$ and $C_yH_{2y-1}^+$ distributions peaked at C_4 or C_5 and C_7, respectively, which were essentially independent of the reactant hydrocarbon ions. On the basis of observed distributions and calculated thermochemical data, it was concluded that the major reactions for the formation of $C_yH_{2y+1}^+$ were proton transfer to a C=C bond and hydride-ion abstraction from the alkyl portion in the CH_5^+ reactions, proton transfer to a C=C bond in the $C_2H_5^+$ reactions, and addition to a C=C bond in the $C_3H_5^+$ reactions, while the major reactions for the formation of $C_yH_{2y-1}^+$ were hydride-ion abstraction in the CH_5^+ reactions, alkanide-ion abstraction in the $C_2H_5^+$ reactions, and addition to a C=C bond in the $C_3H_5^+$ reactions.

The gas phase ion-molecule reactions of 1-olefins in a methane atmosphere have been extensively studied since the first chemical ionization (CI) mass spectrometric measurements by Field et al.[1–4] They measured CI mass spectra of 1-olefins (C_xH_{2x}: x = 6–10, 12, 16, 20) at a medium CH_4 pressure of 1 Torr (= 133.33 Pa), where dominant reactant ions were CH_5^+ (48%), $C_2H_5^+$ (40%), and $C_3H_5^+$ (6%).[5] The spectra consisted of alkyl $C_yH_{2y+1}^+$ (y = 3–x) and alkenyl $C_yH_{2y-1}^+$ (y = 4–x) ions. In this work, x represents the number of carbons of reagent 1-olefin, while y stands for the number of carbons of fragment alkyl and alkenyl ions. Field[1] reported that the attack of the reactant ions upon 1-olefins does not occur randomly over the structures of the molecules. Alkyl $C_yH_{2y+1}^+$ (y = 3–x) ions are produced from the olefins only by proton addition to the olefin portion of molecule, while alkenyl $C_yH_{2y-1}^+$ (y = 4–x) ions are formed by attack of the reactant ions upon the alkyl portion of the olefins via hydride-ion or alkanide-ion abstraction reactions. Therefore, he suggested that the sum of the intensities of the alkyl ions serves as a measure of the attack at the double bond, while the sum of the intensities of the alkenyl ions serves as a measure of the attack of the reactant ions on the alkyl portion of 1-olefins. He postulated that for the smaller olefins attack at the double bond predominates, but as the size of the alkyl group becomes larger an increasing amount of attack along the side chain occurs. Since the reactant ions have not been separated in his CI experiments, the contribution of each hydrocarbon ion to the formation of alkyl and alkenyl ions has not been determined.

Houriet and Gäumann[6] have reported the CI mass spectra of C_7–C_9 1-olefins using H_2O, CH_4, CD_4, or CD_3OD as ionizing gas. They observed $C_xH_{2x+1}^+$, $C_xH_{2x}^+$, $C_xH_{2x-1}^+$, $C_yH_{2y+1}^+$, and $C_yH_{2y-1}^+$ ions, when CH_4 was used as a CI gas. On the basis of the energetics and isotope effects, the reaction mechanism of the CH_4^+, CH_5^+, and $C_2H_5^+$ reactions with 1-olefins were discussed. However, detailed information on the reaction mechanism was not obtained, because the reactant ions were not separated. Budzikiewicz and Busker[7] have reported the isobutane CI mass spectra of octadecenes. The spectra were similar to the CH_4 CI mass spectra in showing $C_yH_{2y+1}^+$ (y = 5–x) and alkenyl $C_yH_{2y-1}^+$ (y = 5–x) ions. In addition, a prominent $[C_{18}H_{36} + C_4H_9]^+$ adduct ion was observed.

Recently, the ion-trap detector (ITD), which can operate at much lower CI gas pressures than those in conventional medium-pressure CI mass spectrometer, has been used as a new sensitive CI mass spectrometer.[9–11] Some comparative studies between medium-pressure CI using magnetic sector instruments and low-pressure CI in the ITD have been carried out.[9–11] In general, fragmentation increases and no adduct ions such as $(M + C_2H_5)^+$ and $(M + C_3H_5)^+$ are observed in the ITD. These facts were explained by the lack of collisional stabilization of $(M + H)^+$, $(M + C_2H_5)^+$, and $(M + C_3H_5)^+$ ions due to secondary collisions with CH_4 and He gases. The other reason for the higher fragmentation in the ion-trap experiments is higher kinetic energies of reactant ions.

All of previous medium-pressure CH_4 CI mass studies on 1-olefins have been carried out without selecting reactant hydrocarbon ions. Therefore, the reactivity of dominant CH_5^+ and $C_2H_5^+$ reactant ions for 1-olefins has not been determined. It is known that $C_3H_5^+$ ion is involved as a minor reactant ion when CH_4 was used as a CI gas. However, no information has been obtained on its reactivity for 1-olefins.

In this study, CH_4 CI mass spectra of a series of 1-olefins (C_xH_{2x}: x = 8–18) by the CH_5^+, $C_2H_5^+$, and $C_3H_5^+$ ions are measured under a reactant-ion selective mode of an ion-trap

type of GC/MS. The dependence of product-ion distributions on the reaction time was measured and compared with the previous data of Field et al.[1–4] in order to examine the effects of collisional stabilization and kinetic energies of reactant ions. The reactivity of CH_5^+, $C_2H_5^+$, and $C_3H_5^+$ for 1-olefins was discussed from the product-ion distributions. Preliminary results for some 1-olefins (x = 15–18) have been communicated.[12]

Experimental

CI mass spectra were obtained using an ion-trap type of Hitachi M7200 GC/MS under a reactant-ion selective mode. The CI CH_4 gas was introduced directly in an trap cell. The electron-impact ionization on CH_4 provides primary CH_n^+ (n = 2–4) ions. One of the reactant CH_5^+, $C_2H_5^+$, and $C_3H_5^+$ ions produced from the subsequent fast ion-molecule reactions of CH_n^+ (n = 2–4) with CH_4 was selectively trapped as a reactant ion in an ion-trap cell. The time for storing a reactant ion was kept at a constant time of 5 ms. If reactant ions in vibrationally excited levels are formed, they will be thermalized by collisions with CH_4 and He during their trapping time in the cell. The ion-trap cell was kept at ≤ 170 °C. The reagents were diluted in hexane, which has a much shorter retention time than those of 1-olefins, and injected into the GC with a high-purity carrier He gas. The partial pressures of CH_4 and He and in an ion-trap cell were 7×10^{-5} and 5×10^{-5} Torr, respectively. The reaction time corresponding to the residence time in the ion-trap was varied from 0.5 to 40 ms. The mass spectra were measured at low reagent concentrations of about 1000–10000 pg cm^{-3} in order to reduce secondary ion-molecule reactions.

The operating conditions in the ion-trap cell used in this work were significantly different from those of the conventional medium-pressure CI mass spectrometer developed by Field et al.[1–4] In the medium-pressure CI measurements, the typical CH_4 gas pressure was 1 Torr and the residence time of reactant ions in the ionization-reaction chamber was about 10 μs. Field[4] evaluated the total number of collisions of reactant ions with CH_4 during this residence time to be about 200. In the present low-pressure CI measurements, the total number of collisions of a product ion with CH_4 was estimated to be about 1–100 times within the reaction time of 0.5–40 ms from a simple gas-kinetic hard-sphere collision model. CI mass spectra were measured under the conditions where concentrations of reactant ions were much higher than those of product ions. Therefore, it was difficult to determine rate constants from plots of a decay of a reactant ion against the reaction time or the concentration of a reagent.

Results and Discussion

Contribution of Collisional Stabilization and Initial Product-Ion Distributions: When CI mass spectra resulting from ion-molecule reactions of CH_5^+, $C_2H_5^+$, and $C_3H_5^+$ with 1-olefins (C_xH_{2x}: x = 8–18) were measured, alkyl $C_yH_{2y+1}^+$ (y = 3–x) and alkenyl $C_yH_{2y-1}^+$ (y = 3–x) ions were observed. If the collisional stabilization takes part in the formation of product ions, excess energy is partly relaxed by collisions with CH_4 and He gases. Therefore, fragmentation will be suppressed in CI mass spectra obtained at long reaction times. In order to examine the contribution of collisional stabilization in our CI conditions, the dependence of product-ion distributions on the reaction time was measured. Figures 1 and 2 show product-ion distributions of $C_yH_{2y+1}^+$ (y = 3–x) and $C_yH_{2y-1}^+$ (y = 3–x) in each reaction at five different reaction times: 0.5, 2, 10, 20, and 40 ms, respectively. The $C_yH_{2y+1}^+$ (y = 3–x) and $C_yH_{2y-1}^+$ (y

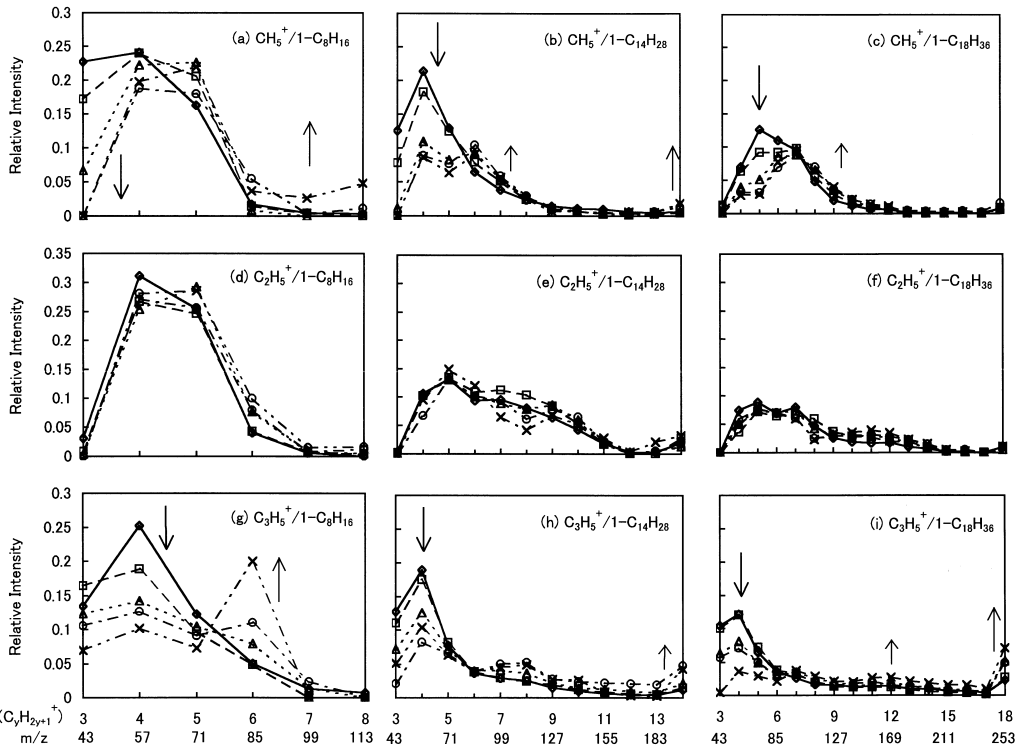

Fig. 1. Dependence of product-ion distributions of alkyl $C_yH_{2y+1}^+$ (y = 3–x) ion on the reaction time in the ion-molecule reactions of CH_5^+, $C_2H_5^+$, and $C_3H_5^+$ with C_8, C_{14}, and C_{18} 1-olefins. Reaction time ◇: 0.5, □: 2, △: 10, ○: 20, and ×: 40 ms. Relative intensities were branching ratios of each ion for total product ions. Arrows indicate an increase or a decrease in product-ion distribution with an increasing the reaction time. The line connecting the points in the graphs is the $C_yH_{2y+1}^+$ formed from the same reaction time.

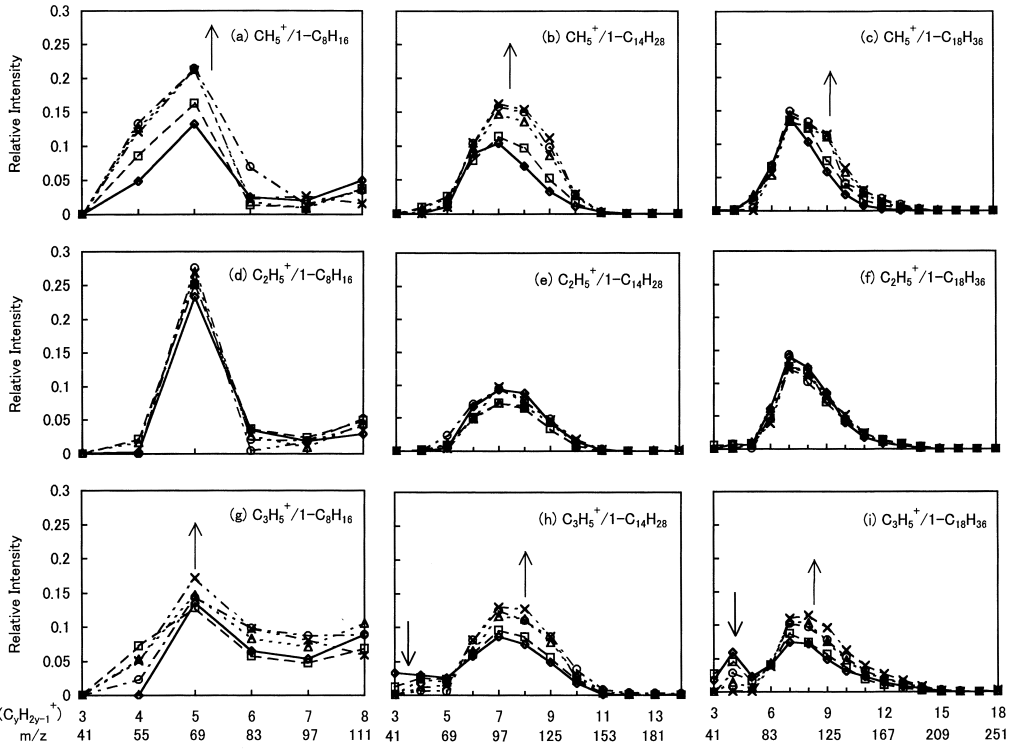

Fig. 2. Dependence of product-ion distributions of alkenyl $C_yH_{2y-1}^+$ ($y = 3$–x) ion on the reaction time in the ion-molecule reactions of CH_5^+, $C_2H_5^+$, and $C_3H_5^+$ with C_8, C_{14}, and C_{18} 1-olefins. Reaction time ◇: 0.5, □: 2, △: 10, ○: 20, and ×: 40 ms. Relative intensities were branching ratios of each ion for total product ions. Arrows indicate an increase or a decrease in product-ion distribution with an increasing the reaction time. The line connecting the points in the graphs is the $C_yH_{2y-1}^+$ formed from same reaction time.

$= 3$–x) distributions exhibit single peaks, except for the $C_yH_{2y-1}^+$ ($y = 3$–x) distributions in the $C_3H_5^+$ reactions, which have second weak peaks at low y values ($y = 3, 4$). It is clear from Figs. 1 and 2 that the $C_yH_{2y+1}^+$ and $C_yH_{2y-1}^+$ distributions depend on the reaction time in most cases, though the changes in the $C_2H_5^+$ reactions are very small in comparison with those in the CH_5^+ and $C_3H_5^+$ reactions. The decreases or increases in the product-ion distributions with increasing the reaction time are shown by arrows in Figs. 1 and 2. In the CH_5^+ and $C_3H_5^+$ reactions, the branching ratios of the small $C_yH_{2y+1}^+$ ($y = 3$–5) fragment ions decrease, while the large $C_yH_{2y+1}^+$ ($y = 6$–x) ions increase with increasing the reaction time. This implies that small $C_yH_{2y+1}^+$ ($y = 3$–5) ions result from dissociation of long-lived precursor $C_xH_{2x+1}^+$ and large $C_yH_{2y+1}^+$ ($y = 6$–x) ions. In the CH_5^+ and $C_3H_5^+$ reactions, the branching ratios of major $C_yH_{2y-1}^+$ peaks having medium y values increase, indicating that they are collisionally stabilized at long reaction times. In the $C_3H_5^+$ reactions, the relative intensities of minor $C_yH_{2y-1}^+$ peaks at $y = 3, 4$ decrease, while those of major $C_yH_{2y-1}^+$ peaks at $y = 6$–x increase. This shows that the former small ions arise from the fragmentation of the latter larger ions. It should be noted that the $\Sigma C_yH_{2y-1}^+$ and $\Sigma C_yH_{2y+1}^+$ values in the CH_5^+ and $C_3H_5^+$ reactions increase by 23–77% due to a significant increase in the medium $C_yH_{2y-1}^+$ ions and decrease by 14–43% due to a significant decrease in the small $C_yH_{2y+1}^+$ ions, respectively, with increasing the reaction time. This implies that small $C_yH_{2y+1}^+$ and medium $C_yH_{2y-1}^+$ ions arise from the same precursor ions in the CH_5^+ and $C_3H_5^+$ reactions, and the collisionally stabilization enhances the $\Sigma C_yH_{2y-1}^+/\Sigma C_yH_{2y+1}^+$ ratios. The initial product-ion distributions were determined by extrapolating the dependence of branching ratios of product ions on the reaction time to zero reaction time, as is shown for the case of the $C_3H_5^+$/1-$C_{14}H_{28}$ reaction in Figs. 3a and 3b. The uncertainties of the initial branching-ratios were estimated to be within ±8%.

Distribution of Alkyl $C_yH_{2y+1}^+$ ($y = 3$–x) Ions: Figures 4a–4i show initial product-ion distributions of $C_yH_{2y+1}^+$ ($y = 3$–x) obtained for short ($x = 8$–10), medium ($x = 11$–14), and long ($x = 15$–18) chain reagents. The $C_yH_{2y+1}^+$ ($y = 3$–x) ions were observed in the CH_5^+, $C_2H_5^+$, and $C_3H_5^+$ reactions. In the CH_5^+ reactions, the intensity distributions peak at $y = 3$ for the short-chain $x = 8$, 9 reagents and the maximum distributions shift to $y = 4$ for the medium chain $x = 10$–14 reagents. For the long-chain $x = 15$–18 reagents, the maximum distributions shift to $y = 5$ and the peaks at $y = 5$ monotonically decrease with increasing the reagent chain-length. Although the $C_yH_{2y+1}^+$ ($y = 3$–x) distributions in the $C_2H_5^+$ reactions are similar to those in the CH_5^+ reactions, they are broader than those in the CH_5^+ reactions for long-chain $x = 11$–18 reagents. Therefore, the relative intensities of $C_yH_{2y+1}^+$ peaks at $y = 5$ decrease, while those of large $C_yH_{2y+1}^+$ ($y = 7$–x) ions become larger in the $C_2H_5^+$ reactions. It should be noted that the $C_yH_{2y+1}^+$ distributions in the $C_3H_5^+$ reactions become sharp and shift to low y values in comparison with those in the $C_2H_5^+$ and $C_3H_5^+$ reactions. The distributions are nearly the same for all $x = 8$–18 reagents having a sharp peak at $y = 4$.

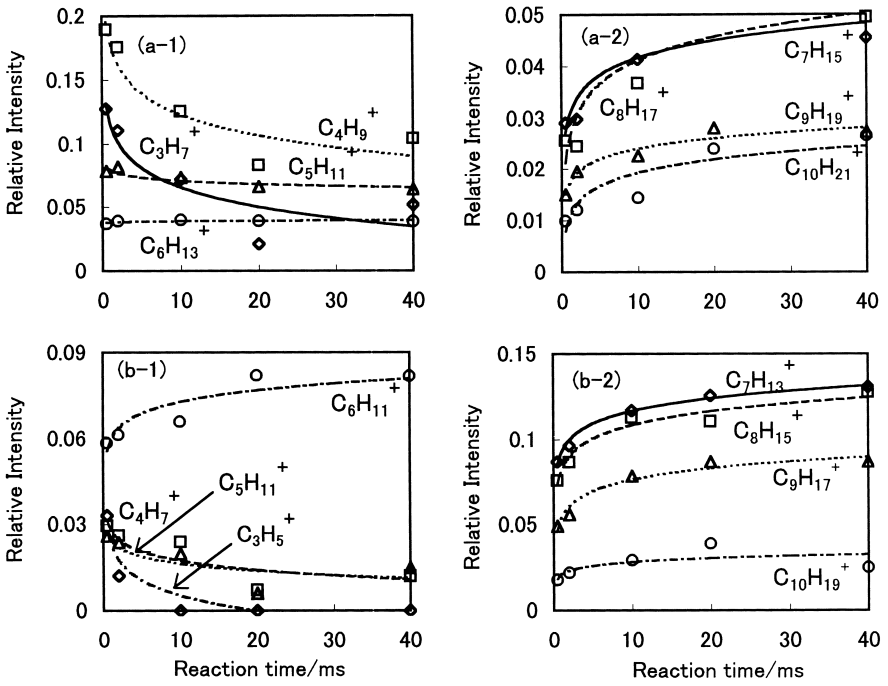

Fig. 3. Dependence of branching ratios of product ions on the reaction time in the $C_3H_5^+$/1-$C_{14}H_{28}$ reactions. (a-1), (a-2): alkyl ion, (b-1), (b-2): alkenyl ion, (a-1) ◇: $C_3H_7^+$, □: $C_4H_9^+$, △: $C_5H_{11}^+$, and ○: $C_6H_{13}^+$. (a-2) ◇: $C_7H_{15}^+$, □: $C_8H_{17}^+$, △: $C_9H_{19}^+$, and ○: $C_{10}H_{21}^+$, (b-1) ◇: $C_3H_5^+$, □: $C_4H_7^+$, △: $C_5H_9^+$, and ○: $C_6H_{11}^+$, (b-2) ◇: $C_7H_{13}^+$, □: $C_8H_{15}^+$, △: $C_9H_{17}^+$, and ○: $C_{10}H_{19}^+$. The lines are extrapolated to zero reaction time to find the initial product-ion distributions.

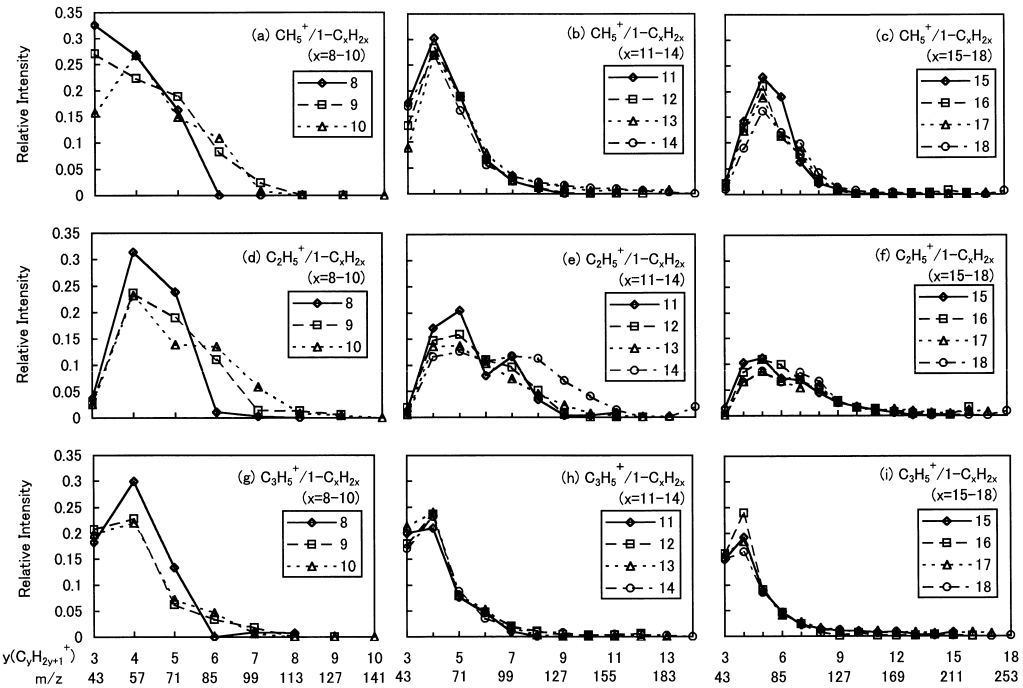

Fig. 4. Initial product-ion distributions of alkyl $C_yH_{2y+1}^+$ ($y = 3–x$) ion in the ion-molecule reactions of CH_5^+, $C_2H_5^+$, and $C_3H_5^+$ with C_8–C_{18} 1-olefins. (a), (d), (g) ◇: C_8H_{16}, □: C_9H_{18}, and △: $C_{10}H_{20}$, (b), (e), (h) ◇: $C_{11}H_{22}$, □: $C_{12}H_{24}$, △: $C_{13}H_{26}$, and ○: $C_{14}H_{28}$ (c), (f), (i) ◇: $C_{15}H_{30}$, □: $C_{16}H_{32}$, △: $C_{17}H_{34}$, and ○: $C_{18}H_{36}$. The line connecting the points in the graphs is the alkyl $C_yH_{2y+1}^+$ ($y = 3–x$) ion formed from the same 1-olefin.

For longer chain $x = 11–18$ reagents, the distributions of long-chain $C_yH_{2y+1}^+$ ($y = 9-x$) ions are nearly zero.

Distribution of Alkenyl $C_yH_{2y-1}^+$ ($y = 3–x$) Ions: Figures 5a–5i show initial product-ion distributions of $C_yH_{2y-1}^+$ (y

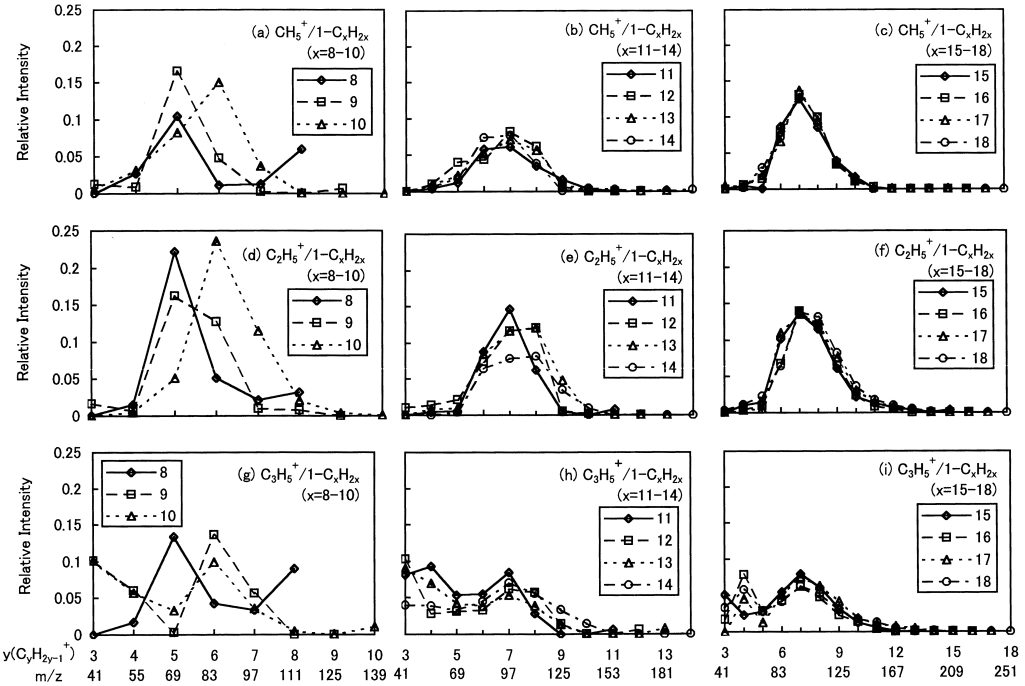

Fig. 5. Initial product-ion distributions of alkenyl $C_yH_{2y-1}^+$ (y = 3–x) ion in the ion-molecule reactions of CH_5^+, $C_2H_5^+$, and $C_3H_5^+$ with C_8–C_{18} 1-olefins. (a), (d), (g) ◇: C_8H_{16}, □: C_9H_{18}, and △: $C_{10}H_{20}$, (b), (e), (h) ◇: $C_{11}H_{22}$, □: $C_{12}H_{24}$, △: $C_{13}H_{26}$, and ○: $C_{14}H_{28}$ (c), (f), (i) ◇: $C_{15}H_{30}$, □: $C_{16}H_{32}$, △: $C_{17}H_{34}$, and ○: $C_{18}H_{36}$. The line connecting the points in the graphs is the alkenyl $C_yH_{2y-1}^+$ (y = 3–x) ion formed from the same 1-olefin.

= 3–x) obtained for short (x = 8–10), medium (x = 11–14), and long (x = 15–18) chain reagents. The $C_yH_{2y-1}^+$ (y = 3–x) ions were observed in the CH_5^+, $C_2H_5^+$, and $C_3H_5^+$ reactions. In the CH_5^+ reactions, the intensity distributions peak at y = 5, 6 for the short-chain x = 8–10 reagents and the maximum distributions shift to y = 7 for the longer-chain x = 11–18 reagents. The $C_yH_{2y-1}^+$ distributions in the $C_2H_5^+$ reactions are very similar to those in the CH_5^+ reactions. The $C_yH_{2y-1}^+$ distributions for x = 11–18 are similar in the CH_5^+ and $C_2H_5^+$ reactions, indicating that the alkenyl-ion distributions are essentially independent of the chain length for x = 11–18 in these reactions. The $C_yH_{2y-1}^+$ distributions in the $C_3H_5^+$ reactions are slightly different from those in the CH_5^+ and $C_2H_5^+$ reactions. In addition to the first main peaks at y = 7, as observed in the CH_5^+ and $C_2H_5^+$ reactions, the second minor peaks at y = 4 appear for long-chain x = 11–18 reagents. Therefore, the relative intensities of the first peaks at y = 7 are smaller than those in the CH_5^+ and $C_2H_5^+$ reactions. The $C_yH_{2y-1}^+$ distributions for x = 11–18 are similar, indicating that the alkenyl-ion distributions are essentially independent of chain length for x = 11–18 in the $C_3H_5^+$ reactions, as in the cases of the CH_5^+ and $C_2H_5^+$ reactions.

Total Alkyl and Alkenyl Ion Intensities: In Figs. 6a–6c we plot the sum of the intensities of all the $C_yH_{2y+1}^+$ (y = 3–x) ions and the sum of intensities of all the $C_yH_{2y-1}^+$ (y = 3–x) ions formed from each of the straight-chain 1-olefins studied. In the CH_5^+ and $C_2H_5^+$ reactions, total alkyl ion intensities decrease, while total alkenyl ion intensities increase with increasing x, being consistent with previous observations of Field[1] without separating the reactant CH_5^+ and $C_2H_5^+$ ions. Field[1] suggested that alkyl $C_yH_{2y+1}^+$ (y = 3–x) ions are produced from the 1-olefins only by proton addition to the olefin molecules, while alkenyl $C_yH_{2y-1}^+$ (y = 4–x) ions are formed by attack of the reactant ions upon the alkyl portion of the 1-olefins via hydride-ion or alkanide-ion abstraction reaction. It is believed that allylic hydrogen is most readily abstracted.[1,8] As the size of the alkyl group becomes larger, an increasing amount of attack along the side chain occurs, so that the $\Sigma C_yH_{2y-1}^+/\Sigma C_yH_{2y+1}^+$ ratios increase. Although the relative contribution between CH_5^+ and $C_2H_5^+$ was not determined in his CI experiment, we found here that the dependence of $\Sigma C_yH_{2y+1}^+$ and $\Sigma C_yH_{2y-1}^+$ on the reagent chain-length was similar for the two reactions. However, the $\Sigma C_yH_{2y-1}^+/\Sigma C_yH_{2y+1}^+$ ratios in the CH_5^+ reactions was about a half of those in the $C_2H_5^+$ reactions for x = 8–18 reagents. It should be noted that the $\Sigma C_yH_{2y+1}^+$ and $\Sigma C_yH_{2y-1}^+$ values remain constant for x = 8–18 reagents in the $C_3H_5^+$ reactions. This different tendency suggests that the reaction mechanisms leading to alkyl and alkenyl ions in the $C_3H_5^+$ reactions are different from those in the CH_5^+ and $C_2H_5^+$ reactions.

Comparison with the Previous CI Experiments: Field[1] measured CI mass spectra of 1-olefins (C_xH_{2x}: x = 6–10, 12, 16, 20) at a medium CH_4 pressure of 1 Torr. For example, his CI mass data of 1-$C_{16}H_{32}$ are shown in Figs. 7a and 7b, along with our corresponding data for the $C_nH_5^+$ (n = 1–3) reactions, in order to examine the effects of collisional stabilization and kinetic energies of reactant ions. The CI mass spectra of Field[1] consisted of alkyl $C_yH_{2y+1}^+$ (y = 3–x) and alkenyl $C_yH_{2y-1}^+$ (y = 4–x) ions, as shown in Figs. 7a and 7b. The $C_yH_{2y+1}^+$ and $C_yH_{2y-1}^+$ distributions in his spectra were similar to those observed here in the $C_2H_5^+$/1-$C_{16}H_{32}$ reactions, except for the appearance of relatively strong $C_{16}H_{31}^+$ and $C_{16}H_{33}^+$ peaks. It is

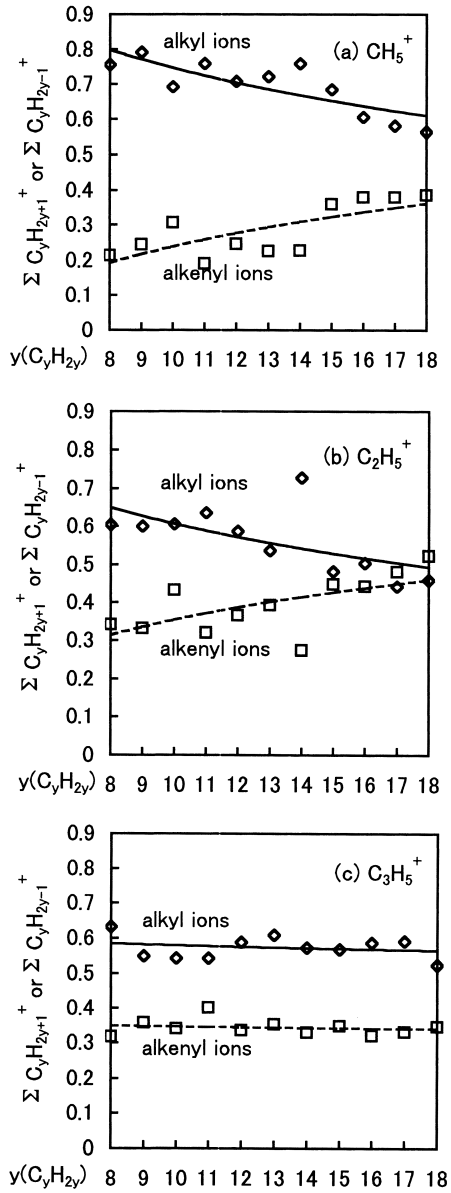

Fig. 6. Total alkyl and alkenyl ion intensities in the reactions of CH_5^+, $C_2H_5^+$, and $C_3H_5^+$ with C_8–C_{18} 1-olefins. ◇: alkyl ion, □: alkenyl ion.

therefore reasonable to assume that the major reactant ion for the formation of product ions was $C_2H_5^+$ in his CI experiment. We found here that the extent of fragmentation in the $C_2H_5^+$/1-$C_{16}H_{32}$ reaction is slightly higher than that observed by Field.[1] One reason for the higher extent of fragmentation observed here will be lack of collisional stabilization under our experimental conditions. The other reason will be the difference in the kinetic energy of reactant ions. The maximum and average kinetic energies of reactant ions in our apparatus were evaluated to be 10 and 4.2 eV for CH_5^+, 6.0 and 2.4 eV for $C_2H_5^+$, and 4.3 and 1.7 eV for $C_3H_5^+$, respectively, using equations reported previously.[13] These energies are higher than those in the medium-pressure CI experiments, which were estimated to be less than 1 eV.[14]

Energetics and Mechanism of Each Ion-Molecule Reaction: Possible formation processes of $C_yH_{2y+1}^+$ and $C_yH_{2y-1}^+$ by the MH^+ (M = CH_4, C_2H_4, and C_3H_4) reactions are shown in Scheme 1. The $C_yH_{2y+1}^+$ alkyl ions can be formed via proton transfer to a C=C double bond (1), hydride-ion abstraction (2a), alkenide-ion abstraction (3a), and adduct-ion formation (4a) and (4b). On the other hand, the $C_yH_{2y-1}^+$ alkenyl ions are produced via hydride-ion abstraction (2b), alkanide-ion abstraction (3b), and adduct-ion formation (4c). The rearrangement shown in Scheme 1 represents hydride and alkyl sifts leading to more stable isomers (e.g. primary → secondary → tertiary ions). It is known that the $C_2H_5^+$/*n*-paraffins reactions leading to $C_yH_{2y+1}^+$ ions proceed exclusively though hydride-ion abstraction:[13]

$$C_2H_5^+ + C_xH_{2x+2} \rightarrow C_xH_{2x+1}^+ + C_2H_6, \quad (5a)$$
$$C_xH_{2x+1}^+ \rightarrow C_yH_{2y+1}^+ + C_{x-y}H_{2(x-y)}. \quad (5b)$$

It should be noted that the intermediate $C_xH_{2x+1}^+$ ions produced from reaction (5a) are the same as those produced from $MH^+ + C_xH_{2x}$ proton-transfer reaction (1). However, no reaction leading to $C_xH_{2x-1}^+$ and $C_yH_{2y-1}^+$ was observed in the $C_2H_5^+$/*n*-paraffins. Therefore, the following proton-transfer reactions by loss of H_2 were excluded from the possible formation processes of $C_yH_{2y-1}^+$:

$$MH^+ + C_xH_{2x} \rightarrow C_xH_{2x+1}^+ + M \quad (M = CH_4, C_2H_4, \text{and } C_3H_4), \quad (6a)$$
$$C_xH_{2x+1}^+ \rightarrow C_xH_{2x-1}^+ + H_2 \quad (6b)$$
$$C_xH_{2x-1}^+ \rightarrow C_yH_{2y-1}^+ + C_{x-y}H_{2(x-y)}. \quad (6c)$$

The energetics of each process for the formation of $C_yH_{2y+1}^+$ and $C_yH_{2y-1}^+$ was calculated using reported thermochemical data.[15] The results obtained are shown in Figs. 8A–8I and 9A–9I for the cases of x = 8, 14, and 18 reagents. Similar energy

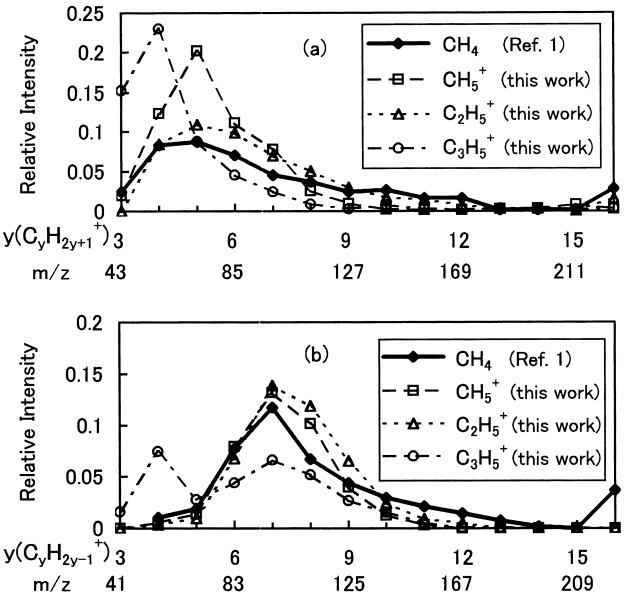

Fig. 7. CH_4 CI mass spectra of 1-$C_{16}H_{32}$ obtained by Field et al. (Ref. 1) in a medium-pressure without selecting reactant ions and initial distributions in the CH_5^+, $C_2H_5^+$, and $C_3H_5^+$ reactions obtained in this study.

(1) Proton transfer by MH^+ (M = CH_4, C_2H_4, and C_3H_4) by loss of alkene

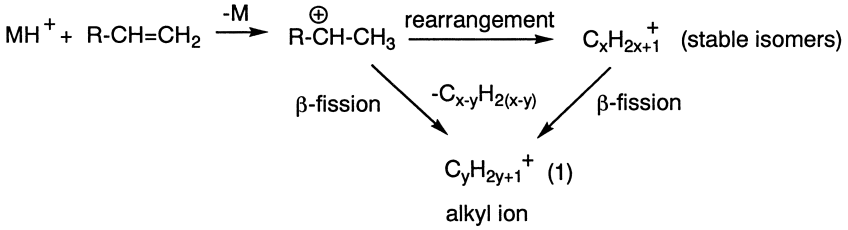

(2) Hydride-ion abstraction by MH^+ (M = CH_4, C_2H_4, and C_3H_4) by loss of diene or alkene

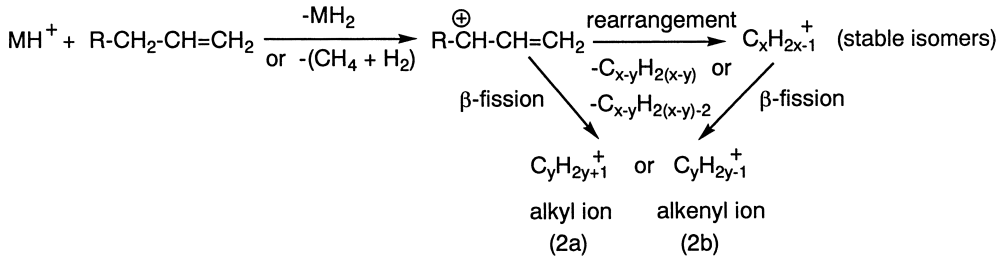

(3) Alkenide- or alkanide-ion abstraction by MH^+ (M = C_2H_4 and C_3H_4)

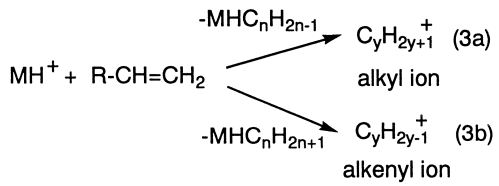

(4) Adduct-ion formation by MH^+ (M = C_2H_4 and C_3H_4)

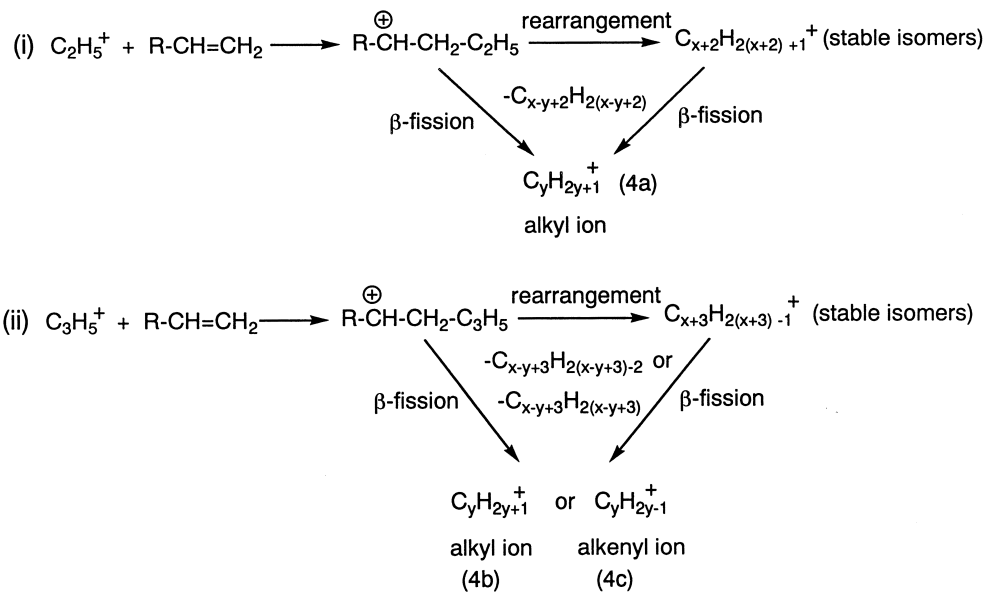

Scheme 1. Possible reaction pathways for the ion-molecule reactions of MH^+ (M = CH_4, C_2H_4, and C_3H_4) with 1-olefins.

relationships are obtained for the reactions of other 1-olefins. For example, ΔH^o values in Fig. 8A represent the heats of reaction of the following CH_5^+/1-C_8H_{16} reactions leading to various $C_yH_{2y+1}^+$ ions:

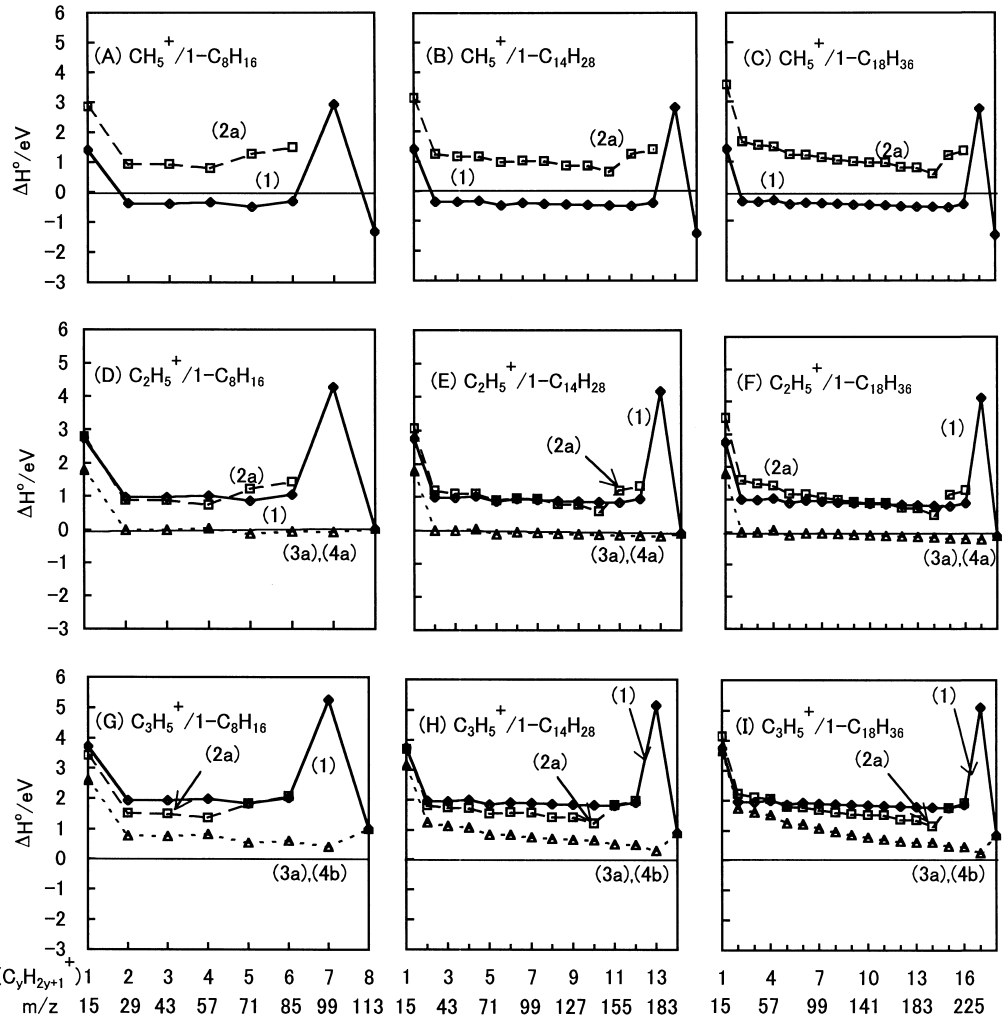

Fig. 8. Energy relations in the ion-molecule reactions of CH_5^+, $C_2H_5^+$, and $C_3H_5^+$ with 1-C_8H_{18}, 1-$C_{14}H_{30}$, and 1-$C_{18}H_{38}$ leading to 1-$C_xH_{2x+1}^+$ and 1-$C_yH_{2y+1}^+$. ◇: (1) Proton transfer, □: (2a) hydride-ion abstraction, △: (3a) alkenide-ion abstraction, (4a), (4b) adduct-ion formation. The largest $C_yH_{2y+1}^+$ ions correspond to the $C_xH_{2x+1}^+$ ions. The line connecting the points in the graphs is the $C_xH_{2x+1}^+$ and $C_yH_{2y+1}^+$ formed from the same reaction pathway. The difference between processes (3a) and (4a), or (3a) and (4b) wasn't described because processes (3a) and (4a), or (3a) and (4b) produce the same product.

$$CH_5^+ + \text{1-}C_8H_{16} \rightarrow C_yH_{2y+1}^+ + C_{8-y}H_{2(8-y)} + CH_4,$$
(process 1 for $x = 8$ in Scheme 1),

$$CH_5^+ + \text{1-}C_8H_{16} \rightarrow C_yH_{2y+1}^+ + C_{8-y}H_{2(8-y)-2} + CH_4 + H_2,$$
(process 2(a) for $x = 8$ in Scheme 1).

There are three possible $C_3H_5^+$ isomers, whose ΔH^o values are 946, 969, and 1069 kJ mol^{-1} for $CH_2{=}CHCH_2^+$, $CH_3C{=}CH_2^+$, and protonated cyclopropene ion, respectively.[15] Since the most stable $CH_2{=}CHCH_2^+$ isomer is a significant ion produced from CH_4 CI gas,[16] all thermochemical calculations for $C_3H_5^+$ are carried out using the above ΔH^o value of $CH_2{=}CHCH_2^+$. The ΔH^o values in Figs. 8A–8I and 9A–9I are calculated for the formation of unstable $-CH_2^+$ (= $C_yH_{2y+1}^+$) and $-CH{=}CH^+$ (= $C_yH_{2y-1}^+$) ions, *n*-paraffins, and 1-olefins as ionic and neutral products. However, more stable isomers having secondary and tertiary alkyl groups will be formed, so that many endoergic processes become possible via stabilization due to intramolecular rearrangement.

It is clear from Figs. 8A–8I that the ΔH^o values for the formation of alkyl $C_yH_{2y+1}^+$ ions are essentially independent of the reagent chain-length x and the product-ion chain-length y, except for the highly endoergic processes for the formation of CH_2^+ and $C_{x-1}H_{2(x-1)+1}^+ + CH_2$. However, the ΔH^o values given in Figs. 8A–8I slightly decrease with increasing y in the $y = 1$–$(x - 2)$ range. The ΔH^o values given in Figs. 8A–8I increase in the order of CH_5^+, $C_2H_5^+$, and $C_3H_5^+$ reactions due to an increase in the proton affinity (PA) in the order of CH_4 (PA = 543.5 kJ mol^{-1}), C_2H_4 (680.5 kJ mol^{-1}), and C_3H_4 (775.3 kJ mol^{-1}).[15] Therefore, more processes become endoergic for larger reactant ions. However, an intramolecular rearrangement makes such processes possible. Figures 9A–9I demonstrate that the ΔH^o values for the formation of alkenyl $C_yH_{2y-1}^+$ ions are essentially independent of the reagent chain-length. The ΔH^o values are highest for the formation of the smallest CH^+ ion and decrease more rapidly than those in the cases of $C_yH_{2y+1}^+$ ions with increasing y. When unstable CH_2 radicals are formed in reaction (2b), the ΔH^o values become

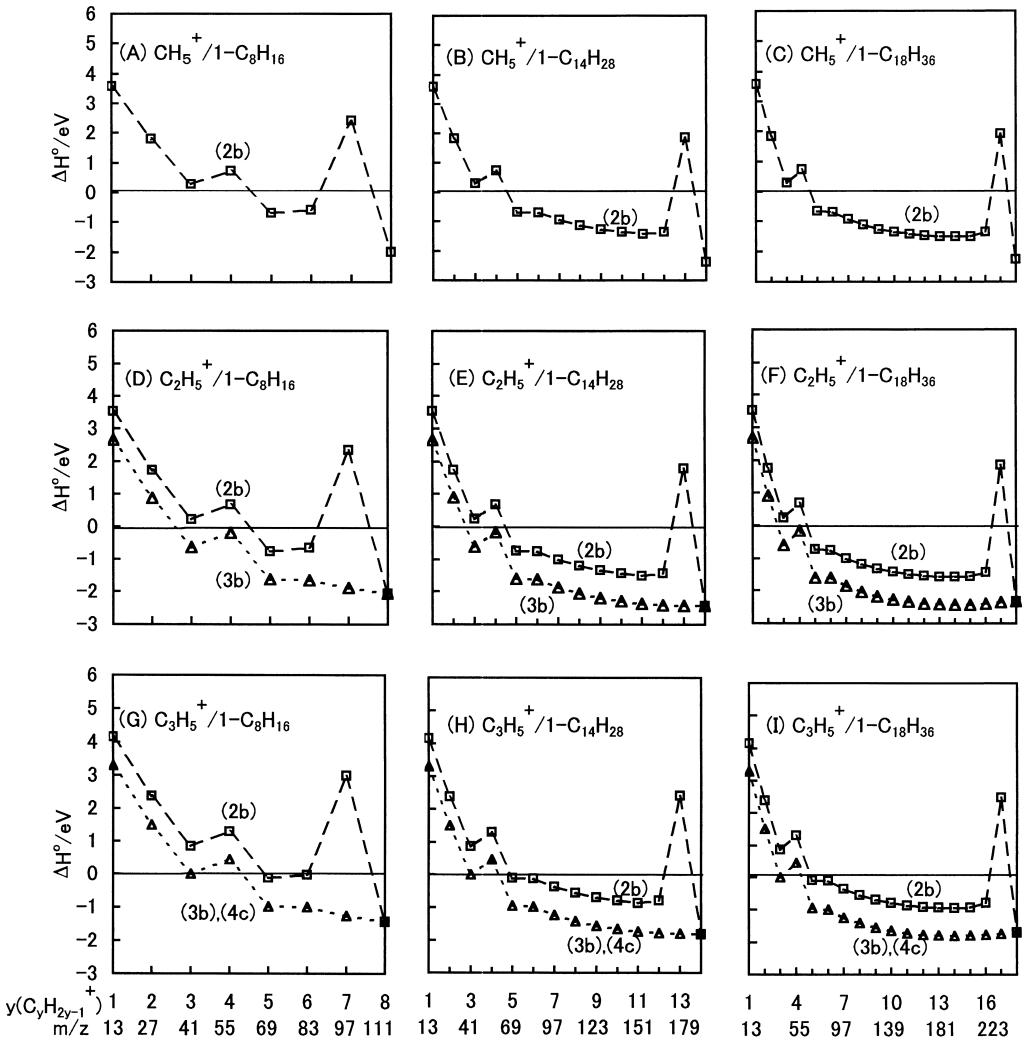

Fig. 9. Energy relations in the ion-molecule reactions of CH_5^+, $C_2H_5^+$, and $C_3H_5^+$ with 1-C_8H_{18}, 1-$C_{14}H_{30}$, and 1-$C_{18}H_{38}$ leading to 1-$C_xH_{2x-1}^+$ and 1-$C_yH_{2y-1}^+$. □: (2b) hydride-ion abstraction, △: (3b) alkanide-ion abstraction, (4c) adduct-ion formation. The largest $C_yH_{2y-1}^+$ ions correspond to the $C_xH_{2x-1}^+$ ions. The line connecting the points in the graphs is the $C_xH_{2x-1}^+$ and $C_yH_{2y-1}^+$ formed from same reaction pathway. The difference between processes (3b) and (4c) wasn't described because processes (3b) and (4c) produce the same product.

very large at $y = x - 1$. It should be noted that all the reactions are exothermic for the formation of $C_yH_{2y-1}^+$ ($y = 5$–$(x - 2)$). The lack of small fragment ions $y < 5$ in the CH_5^+ and $C_2H_5^+$ reactions can be explained by its endoergicity and low possibility of stabilization by rearrangement for short-chain $C_yH_{2y-1}^+$ ions. Figures 8D–8I and Figs. 9D–9I indicate that a significant rearrangement is required for the formation of alkyl $C_yH_{2y+1}^+$ ions in many reactions, while such a rearrangement is unnecessary for the formation of alkenyl $C_yH_{2y-1}^+$ ions.

In the CH_5^+ reactions, $C_yH_{2y-1}^+$ must be formed via process (2b) because it is the only possible process for the formation of $C_yH_{2y-1}^+$. On the other hand, both processes (1) and (2a) are possible for the formation of $C_yH_{2y+1}^+$ in the CH_5^+ reactions. On the basis of energetics, protonation to a C=C bond (1) is more favorable than hydride-ion abstraction (2a). The time dependence of $C_yH_{2y+1}^+$ and $C_yH_{2y-1}^+$ distributions indicated that not only process (1) but also process (2a) takes part in the formation of $C_yH_{2y+1}^+$. The relative contribution of the latter process was estimated to be 14–43%. It is clear from Figs. 8A–8C and Figs. 9A–9C that process (2a) is endoergic, while process (2b) is exothermic in most cases. Therefore, rearrangement from primary to secondary and tertiary $C_yH_{2y+1}^+$ ions is required for the formation of $C_yH_{2y+1}^+$ via process (2a). Such endoergic processes will be suppressed by collisional relaxation of precursor large $C_yH_{2y+1}^+$ ions at long reaction times, while collisional relaxation will have little effect on the formation of small $C_yH_{2y-1}^+$ ions via exothermic processes. Thus, the $\Sigma C_yH_{2y-1}^+/\Sigma C_yH_{2y+1}^+$ ratios increase with increasing the reaction time. The branching ratios of large $C_yH_{2y+1}^+$ ions slightly increase, while those of small $C_{y'}H_{2y'+1}^+$ ($y' < y$) ions decrease with increasing the reaction time in the CH_5^+ and $C_3H_5^+$ reactions, as shown in Figs. 1a–1c and Figs. 1g–1i. This suggests that further fragmentation from large $C_yH_{2y+1}^+$ ions to small $C_{y'}H_{2y'+1}^+$ ions occurs:

$C_yH_{2y+1}^+$ (y = 5–8) → $C_{y'}H_{2y'+1}^+$ (y' = 3,4) + $C_{y-y'}H_{2(y-y')}$ for 1-C_8H_{16}, (7a)

$C_yH_{2y+1}^+$ ($y \geq 6$) → $C_{y'}H_{2y'+1}^+$ (y' = 3–5) + $C_{y-y'}H_{2(y-y')}$ for 1-$C_{14}H_{28}$, (7b)

$C_yH_{2y+1}^+$ ($y \geq 8$) → $C_{y'}H_{2y'+1}^+$ (y' = 3–6) + $C_{y-y'}H_{2(y-y')}$ for 1-$C_{18}H_{36}$. (7c)

These secondary fragmentation processes are collisionally suppressed at long reaction times.

In the $C_2H_5^+$ reactions, $C_yH_{2y+1}^+$ can be formed via processes (1), (2a), (3a), and (4a), and $C_yH_{2y-1}^+$ can be produced via (2b) and (3b). The $C_yH_{2y+1}^+$ and $C_yH_{2y-1}^+$ distributions in the $C_2H_5^+$ reactions are similar to those in the CH_5^+ reactions, though the $C_yH_{2y+1}^+$ distributions are broader. The $\Sigma C_yH_{2y+1}^+$ and $\Sigma C_yH_{2y-1}^+$ values decrease and increase, respectively, with increasing the chain length, as in the case of the CH_5^+ reactions, indicating active sites for the formation of $C_yH_{2y+1}^+$ and $C_yH_{2y-1}^+$ are a C=C double bond and an alkyl chain, respectively. The energetics of processes (2a) and (2b) in the $C_2H_5^+$ reactions are similar to that in the CH_5^+ reactions, as shown in Figs. 8A–8F and 9A–9F. Therefore, if processes (2a) and (2b) participate in the formation of $C_yH_{2y+1}^+$ and $C_yH_{2y-1}^+$, a similar decrease or increase in the branching ratios of $C_yH_{2y+1}^+$ and $C_yH_{2y-1}^+$ will be found in the reaction-time dependence. The lack of significant reaction-time dependence of the branching ratios of $C_yH_{2y+1}^+$ and $C_yH_{2y-1}^+$ suggests that processes (2a) and (2b) are unimportant in the $C_2H_5^+$ reactions. The remaining alkanide-ion abstraction process (3b) will be most significant for the formation of $C_yH_{2y-1}^+$ ions.

Processes (1), (3a), and (4a) are possible for the formation of $C_yH_{2y+1}^+$ in the $C_2H_5^+$ reactions, because process (2a) can be excluded from responsible reactions. The alkenide-ion abstraction process (3a) is energetically unfavorable in comparison with the competitive alkanide-ion abstraction process (3b). In our previous studies of the reactions of $C_2H_5^+$ with monosubsituted benzenes, proton transfer to unsaturated bonds predominates over the association and alkanide-ion abstraction reactions.[17–20] The dependence of branching ratios of $\Sigma C_yH_{2y+1}^+$ and $\Sigma C_yH_{2y-1}^+$ on the chain length in the $C_2H_5^+$ reactions are different from those in the $C_3H_5^+$ reactions, where the association is a dominant process, as discussed in the next paragraph. On the basis of these facts, it is reasonable to assume that process (1) is the major process for the formation of $C_yH_{2y+1}^+$ in the $C_2H_5^+$ reactions. The fact that the $\Sigma C_yH_{2y-1}^+/\Sigma C_yH_{2y+1}^+$ ratios in the $C_2H_5^+$ reactions are higher than those in the CH_5^+ reactions implies that relative reaction rates of alkanide-ion abstraction process (3b) to the proton-transfer process (1) in the $C_2H_5^+$ reactions are larger than those of hydride-ion abstraction process (2b) to proton-transfer process (1) and hydride-ion abstraction process (2a) in the CH_5^+ reactions.

In the $C_3H_5^+$ reactions, $C_yH_{2y+1}^+$ can be formed via processes (1), (2a), (3a), and (4b), and $C_yH_{2y-1}^+$ can be produced via (2b), (3b), and (4c). The $C_yH_{2y+1}^+$ distributions in the $C_3H_5^+$ reactions shift to lower y values than those in the CH_5^+ and $C_2H_5^+$ reactions, though excess energies for proton-transfer process (1) are lower than those in the CH_5^+ and $C_2H_5^+$ reactions. This implies that process (1) is insignificant in the $C_3H_5^+$ reactions. The $C_yH_{2y-1}^+$ distributions in the $C_3H_5^+$ reactions are similar to those in the CH_5^+ and $C_2H_5^+$ reactions, though a second peak appears at a low y = 4 value. The most significant finding observed in the dependence of branching ratios of $\Sigma C_yH_{2y+1}^+$ and $\Sigma C_yH_{2y-1}^+$ on the chain length was that they were essentially independent of the chain length. According to our previous studies on the $C_3H_5^+$ reactions with benzene monoderivatives,[17–20] association processes are often observed as a major exit channel in the $C_3H_5^+$ reactions. It was explained by higher PA and the delocalization of a positive charge, which reduce the probability of proton transfer channels.[17–20] On the basis of the above results, it was concluded that association processes (4b) and (4c) are dominantly responsible for the formation of $C_yH_{2y+1}^+$ and $C_yH_{2y-1}^+$ in the $C_3H_5^+$ reactions.

The time dependence of $C_yH_{2y+1}^+$ and $C_yH_{2y-1}^+$ distributions indicated that small $C_{y'}H_{2y'+1}^+$ and $C_{y'}H_{2y'-1}^+$ ions arise from secondary fragmentation of larger $C_yH_{2y+1}^+$ and $C_yH_{2y-1}^+$ ions: e.g.,

$C_yH_{2y+1}^+$ ($y > 7$) → $C_{y'}H_{2y'+1}^+$ (y' = 4,5) + $C_{y-y'}H_{2(y-y')}$, (8a)

$C_yH_{2y-1}^+$ (y = 6–10) → $C_{y'}H_{2y'-1}^+$ (y' = 4) + $C_{y-y'}H_{2(y-y')}$. (8b)

In addition, we found that the relative formation rates of alkenyl ions to those of alkyl ions increase by collisional relaxation of precursor $(C_3H_5 + C_xH_{2x})^+$ ion. Since the formation of alkyl ions are endoergic, some isomerization must occur. On the other hand, the formation of alkenyl ions are exoergic. The collisional relaxation of precursor $(C_3H_5 + C_xH_{2x})^+$ ion will reduce the probability of endoergic channels. Therefore, the branching ratios of alkenyl ions increase by collisional relaxation.

Concluding Remarks: The gas-phase ion-molecule reactions of CH_5^+, $C_2H_5^+$, and $C_3H_5^+$ with 1-olefins (C_xH_{2x}: x = 8–18) have been studied in an ion-trap type of GC/MS by separating each reactant ion. In all the reactions, alkyl $C_yH_{2y+1}^+$ and alkenyl $C_yH_{2y-1}^+$ (y = 3–x) ions were observed. The dependence of the relative intensities of $C_yH_{2y+1}^+$ and $C_yH_{2y-1}^+$ on the reaction times indicated that collisional stabilization took part in the formation of some product ions. The total alkyl and alkenyl ion intensities decreased and increased with increasing the reagent chain-length in the CH_5^+ and $C_2H_5^+$ reactions, while they were independent of the chain length in the $C_3H_5^+$ reactions. Summarizing the above results, the product-ion distributions, and the energetics, one can conclude that major reactions for the formation of $C_yH_{2y+1}^+$ and $C_yH_{2y-1}^+$ depend on the reactant ion. The dominant formation processes of alkyl ions were proton transfer to a C=C bond and hydride-ion abstraction from the alkyl portion in the CH_5^+ reactions, proton transfer to a C=C bound in the $C_2H_5^+$ reactions, and adduction to a C=C bound in the $C_3H_5^+$ reactions, while major reactions for the formation of alkenyl ions were hydride-ion abstraction in the CH_5^+ reactions, alkanide-ion abstraction in the $C_2H_5^+$ reactions, and adduction to a C=C bound in the $C_3H_5^+$ reactions. The dependence of $C_yH_{2y+1}^+$ and $C_yH_{2y-1}^+$ distributions on the reactant ion and the reagent-chain length was small for x = 11–18. The $C_yH_{2y+1}^+$ distributions peaked at low C_4 or C_5 and the $C_yH_{2y-1}^+$ distributions peaked at C_7. The same stable C_4 and C_5 alkyl ions and C_7 alkenyl ions were probably formed from the reactions of $C_nH_5^+$ (n = 1–3) ions with C_{11}–C_{18} 1-olefins, although further experimental and the-

oretical studies are required for the determination of molecular structures of C_4 and C_5 alkyl ions and C_7 alkenyl ions. Since the formation of such stable alkyl and alkenyl ions is unfavorable for short-chain C_8–C_{10} 1-olefins, smaller fragment alkyl and alkenyl ions are observed as major products. The present results provide new information on the reactivity of hydrocarbon ions for olefins; they are important in understanding organic reactions by carbocations.

The authors acknowledge financial support from the Mitsubishi Foundation and a Grant-in-Aid for Scientific Research No. 09440201 from the Ministry of Education, Science, Sports and Culture.

References

1 F. H. Field, *J. Am. Chem. Soc.*, **99**, 5649 (1968).

2 F. H. Field, M. S. B. Munson, and D. A. Becker, "Advances in Chemistry Series," No. 58, Am. Chem. Soc., Washington, D.C. (1966), pp. 167–192.

3 F. H. Field, in "Mass Spectrometry," MTP Intern. Rev. Sci., Phys. Chem. Ser. 1, ed by Maccoll, Butterworths, London (1972), Vol. 5, pp. 133–181.

4 F. H. Field, in "Ion-Molecule Reactions," ed by J. L. Franklin, Plenum Press, New York (1972), Vol. 1, pp. 261–313.

5 M. S. B. Munson and F. H. Field, *J. Am. Chem. Soc.*, **89**, 1047 (1967).

6 R. Houriet and T. Gäumann, *Helv. Chim. Acta*, **59**, 107 (1976).

7 H. Budzikiewicz and E. Busker, *Tetrahedron*, **36**, 255 (1980).

8 "Chemical Ionization Mass Spectrometry," 2nd ed, ed by A. G. Harrison, CRC Press, Inc., Boca Raton, Florida (1992), pp. 115–118.

9 R. E. Mather and J. F. J. Todd, *Int. J. Mass Spectrom. Ion Process.*, **30**, 1 (1979).

10 J. S. Brodbelt, J. N. Louris, and R. G. Cooks, *Anal. Chem.*, **59**, 1278 (1987).

11 S. M. Boswell, R. E. Mather, and J. F. J. Todd, *Int. J. Mass Spectrom. Ion Process.*, **99**, 139 (1990).

12 M. Tsuji, Y. Tanaka, T. Arikawa, and Y. Nishimura, *Chem. Lett.*, **2000**, 892.

13 Y. Tanaka, M. Tsuji, and Y. Nishimura, *Bull. Chem. Soc. Jpn.*, **73**, 2703 (2000).

14 C. Chang, G. G. Meisels, and J. A. Taylor, *Int. J. Mass Spectrom. Ion Phys.*, **12**, 411 (1973).

15 S. G. Lias, J. E. Bartmess, J. F. Liebman, J. L. Holmes, R. D. Levin, and W. G. Mallard, *J. Phys. Chem. Ref. Data*, **17**, Suppl. 1 (1988); Updated data were obtained from NIST Standard Ref. Database, Number 69, 2000, (http://webbook.nist.gov/chemistry).

16 R. Houriet, T. A. Elwood, and J. H. Futrell, *J. Am. Chem. Soc.*, **100**, 2320 (1978).

17 M. Tsuji and Y. Nishimura, *Bull. Chem. Soc. Jpn.*, **71**, 273 (1998).

18 M. Tsuji, T. Arikawa, and Y. Nishimura, *Bull. Chem. Soc. Jpn.*, **72**, 293 (1999).

19 M. Tsuji, T. Arikawa, and Y. Nishimura, *Bull. Chem. Soc. Jpn.*, **73**, 131 (2000).

20 M. Tsuji, T. Arikawa, Y. Tanaka, and Y. Nishimura, *Bull. Chem. Soc. Jpn.*, **73**, 1673 (2000).